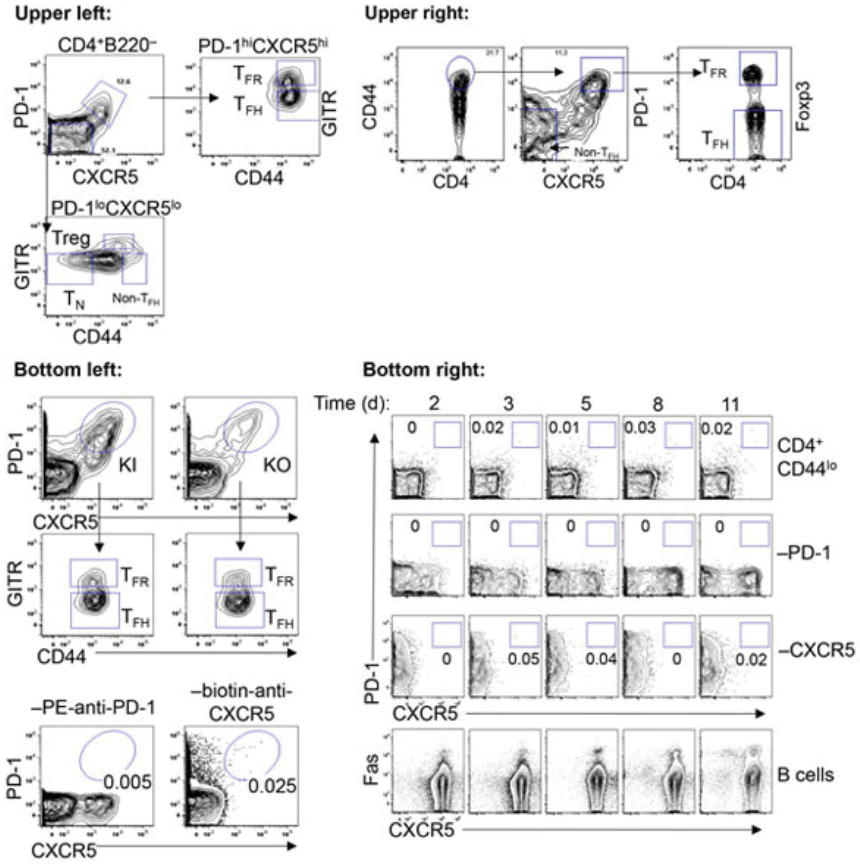

Supplementary Figure 1

Sorting and gating strategy.

Upper left, FACS plots show isolation of different $CD4^+$ T_H populations from B6 or OPN-i-KI mice after immunization with KLH in CFA. T_N: $CD4^+CD44^{lo}CXCR5^{lo}PD\text{-}1^{lo}GITR^-$ naïve cells; T_{FH}: $CD4^+CD44^{hi}CXCR5^+PD\text{-}1^+GITR^-$ cells; T_{FR}: $CD4^+CD44^{hi}CXCR5^+PD\text{-}1^+GITR^+$ cells; Non-T_{FH}: $CD4^+CD44^{hi}CXCR5^{lo}PD\text{-}1^{lo}GITR^-$ cells; T_{reg}: $CD4^+CD44^{med}CXCR5^-PD\text{-}1^-GITR^+$ cells. *Bottom left*, FACS plots show isolation of $CD4^+$ T_{FH} or T_{FR} cells from OPN-i-KI or OPN-KO mice 5 d after immunization with KLH in CFA, shown in Fig. 2e. Gating control stains that lack (–) either anti-PD-1 or biotin-anti-CXCR5 using OPN-i-KI cells are shown. *Upper right*, gating strategy for T_{FH} ($CD4^+CD44^{hi}CXCR5^+PD\text{-}1^+Foxp3^-$), T_{FR} ($CD4^+CD44^{hi}CXCR5^+PD\text{-}1^+Foxp3^+$) and non-$T_{FH}$ ($CD4^+CD44^{hi}CXCR5^{lo}PD\text{-}1^{lo}$) cells in Fig. 3a. *Bottom right*, Gating controls for defining the $PD\text{-}1^+CXCR5^+$ surface phenotype of $CD4^+$ T_{FH} and T_{FR} cells in Fig. 3c. Negative control: $CD4^+CD44^{lo}$ cells; Positive control (for CXCR5 stains): Fas^+B220^+ B cells; FMO PD-1 control: all antibodies except (–) anti-PD-1; CXCR5 control: all antibodies except (–) biotin-anti-CXCR5 (streptavidin-APC alone).

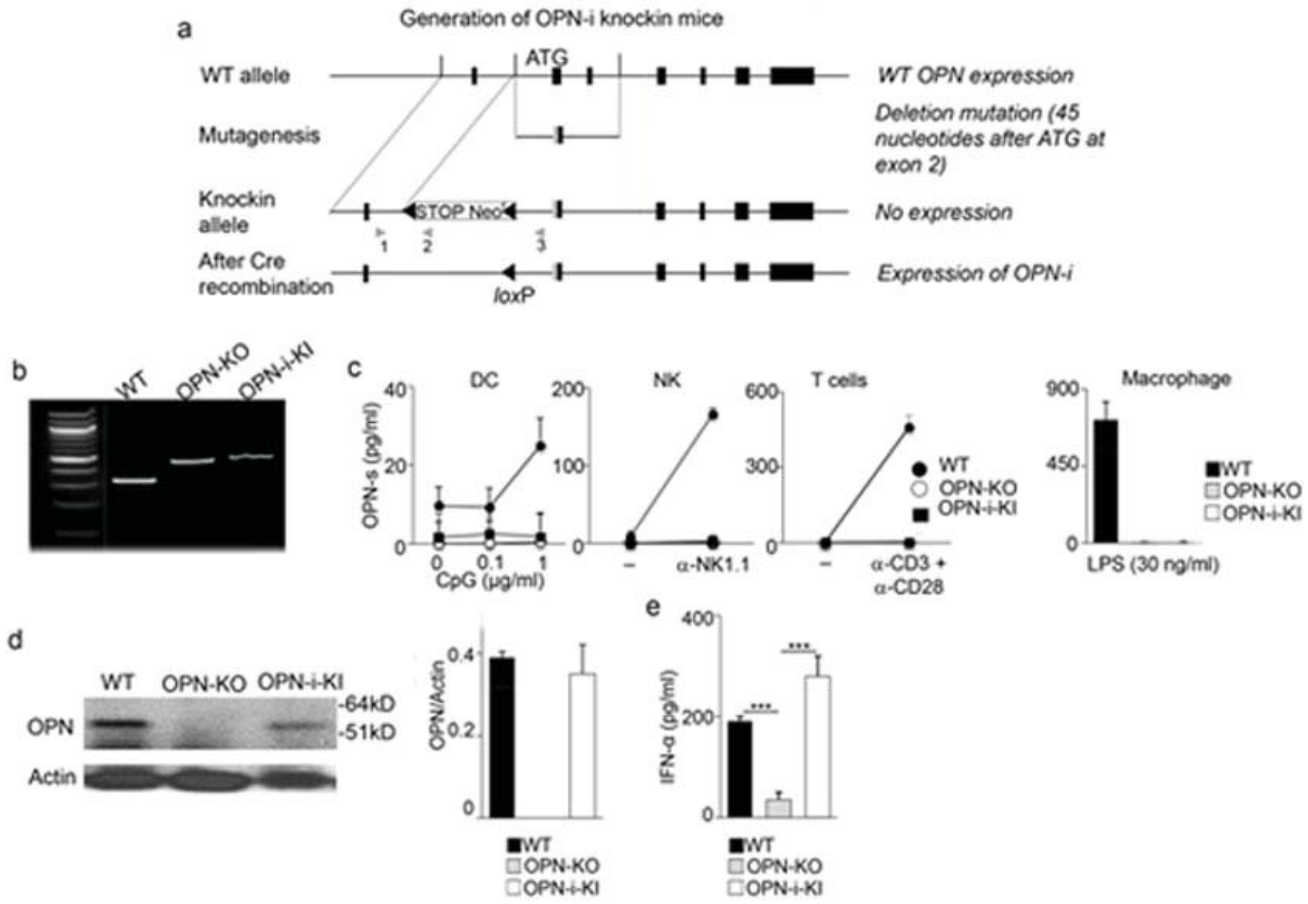

Supplementary Figure 2

Generation and confirmation of OPN-i-KI mice.

a, *Spp1* genomic locus and targeting strategy. Boxes represent exons; exon 2 (gray) indicates the mutation site with deletion of the 45 nucleotides after the translational start site (ATG) that encode an N-terminal signal sequence while sparing other endogenous elements. A transcriptional STOP element flanked by *lox*P sites (black triangles) was inserted upstream of this mutation site to prevent OPN-i expression. Germline transmitted *Spp1*$^{flstop/+}$ mice were backcrossed to B6 mice for at least 5 generations before crossing with mice carrying the Cre recombinase to allow OPN-i expression. neo^{r}, neomycin-resistance gene. **b**, PCR of genomic DNA showing wild-type, OPN-i-KI and OPN-KO mice after crossing with EIIa-Cre mice using genotyping primers indicated as gray triangles in **a**. OPN-KO mice gained the STOP element (194 bp) compared to wild-type allele. wild-type: 324 bp, OPN-i-KI (after Cre recombination): 453 bp, OPN-KO: 518 bp. **c**, Secreted OPN protein measured by ELISA from supernatants of purified DC, NK, T cells and peritoneal macrophages from each mouse strain after stimulation with the indicated reagents for 24 h or 2 d for macrophages. **d**, Immunoblot analysis of splenocyte lysates from the indicated mouse strains, probed with anti-OPN and anti-actin. Right, quantification of ratio of OPN to actin (n = 5 mice per group). **e**, Secreted IFN-α protein in pDC after stimulation by CpG-B (ODN-1668) (n = 3 mice per group) (***$P < 0.001$; error bars, mean ± s.e.m).

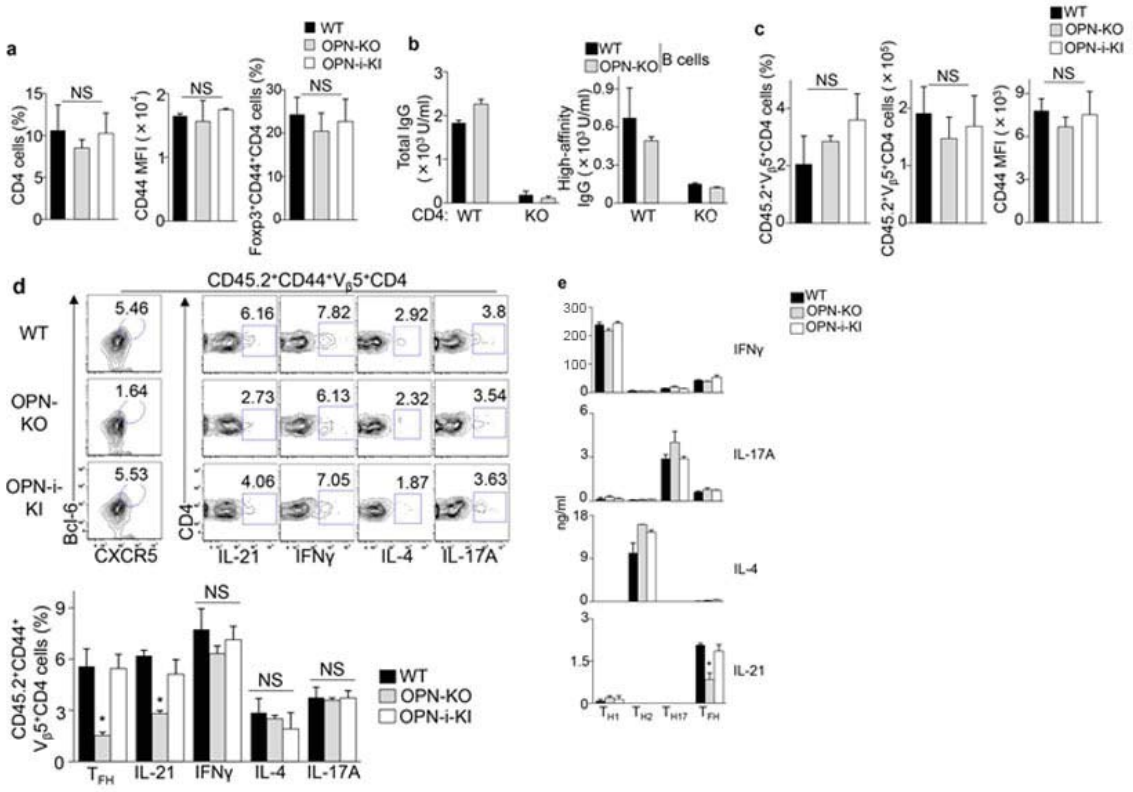

Supplementary Figure 3

OPN-i deficiency does not affect B cell activity or other helper T cell differentiation.

a, Quantification of CD44 expression (MFI) by $CD4^+$ T cells, percent $CD4^+$ T cells and $Foxp3^+CD44^+CD4^+$ T_{reg} cells from OT-II, OT-II OPN-KO and OT-II OPN-i-KI mice (as in **Fig. 1b**) 7 d post-challenge. Data represent at least three independent experiments with 6 mice per group (error bars, mean and ± s.e.m). **b**, Titer of total (NP_{23}) and high-affinity (NP_4) NP-specific IgG in the serum of *Rag2*$^{-/-}$*Prf1*$^{-/-}$ hosts transferred with OT-II $CD4^+$ T cells from OPN wild-type or OPN-KO mice and OPN wild-type or OPN-KO B cells followed by immunization with NP_{13}-OVA in CFA and analysis 10 d later. Data represent two independent experiments with 4 mice per group. **c**, Frequency and numbers of donor $CD45.2^+V_\beta5^+CD4^+$ T cells and surface expression of CD44 by these cells from spleens of CD45.1 congenic recipients 7 d post-immunization with OVA in CFA. **d**, Flow cytometry of donor $V_\beta5^+CD4^+$ T cells in **c**. Numbers adjacent to outlined areas indicate percent $Bcl\text{-}6^+CXCR5^+$ T_{FH} cells and $V_\beta5^+CD4^+$ T cells expressing intracellular cytokines. Below, frequency of T_{FH} cells and cytokine-producing cells (n = 6 mice per group). *$P < 0.05$ (unpaired two-tailed Student's t-test); NS, not significant. Error bars indicate mean ± s.e.m. **e**, Cytokine production by naïve $CD44^{lo}CD25^-CD4^+$ T cells purified from the indicated OT-II mice and differentiated for 5 d under T_H1, T_H2, T_H17 and T_{FH} conditions. *$P < 0.05$ (error bars, mean ± s.e.m of triplicate wells).

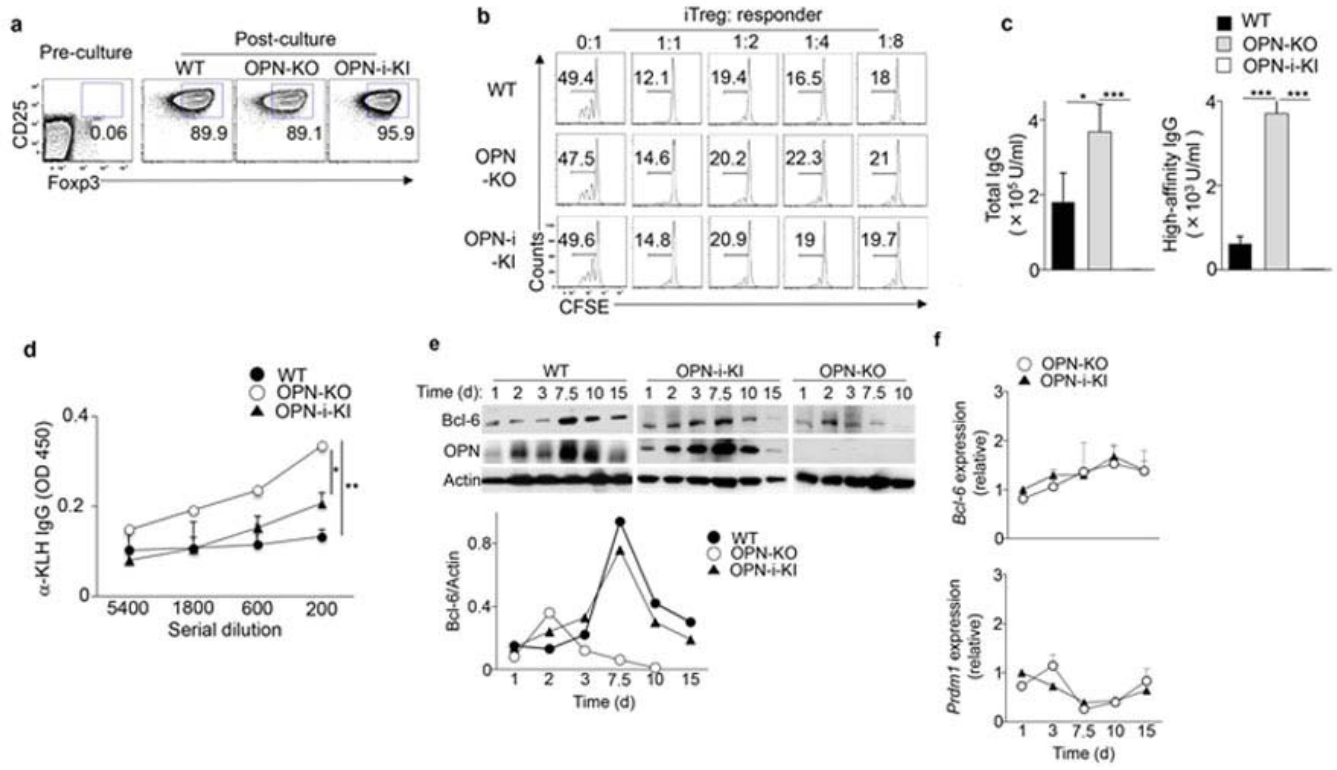

Supplementary Figure 4

Effects of OPN-i deficiency on Bcl-6 expression and the differentiation of inducible T_{reg} cells and T_{FR} cells.

a, Flow cytometry of $CD25^+Foxp3^+$ iT_{reg} differentiated from sorted naïve $CD25^-CD4^+$ T cells, stimulated with plate-bound anti-CD3 (2 μg/ml) and anti-CD28 (1 μg/ml) in the presence of TGF-β1 (5 ng/ml) and hIL-2 (100 U/ml) for 5 d. **b**, iTregs from (**a**) were co-cultured with CFSE-labeled naïve $CD25^-CD4^+$ T cells (responder) activated with anti-CD3 and irradiated APC at different ratios. Histograms of CFSE dilutions, analyzed by flow cytometry, as readout of responder proliferation. Serum titers of total (NP_{23}) and high-affinity (NP_4) IgG (**c**) and anti-KLH (**d**) IgG from recipients in **Fig. 2c** (n = 5 mice per group). $^*P < 0.05$, $^{**}P < 0.01$ and $^{***}P < 0.001$ (unpaired two-tailed Student's t-test; error bars, mean ± s.e.m). **e**, Immunoblot analysis of enriched $CD44^+CD4^+$ T cells from the indicated mice at days 1-15 after immunization with KLH in CFA, probed with the indicated Abs. Below, ratio of Bcl-6 to actin. **f**, RT-PCR analysis of *Bcl6* and *Prdm1* mRNA in $CD44^+CD4^+$ T cells purified from OPN-i-KI or OPN-KO mice from **e**. *Bcl6* or *Prdm1* expression was normalized to the *Rps18* control and results are presented relative to that of OPN-i-KI mice at d1, set as 1. Data are representative of two independent experiments (**e**) or one experiment with 3 mice per time point (**f**; error bars, mean ± s.e.m).

a

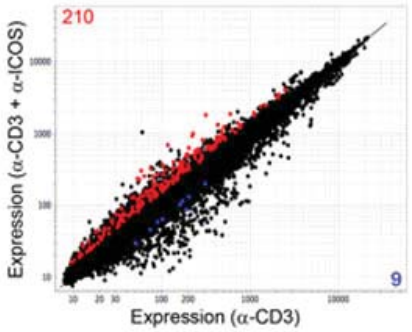

b

Function Annotation	p-value	# Molecules
quantity of T lymphocytes	3.89E-14	26
quantity of B lymphocytes	7.06E-12	19
proliferation of T lymphocytes	8.68E-12	24
systemic autoimmune syndrome	2.65E-11	31
activation of T lymphocytes	3.02E-10	17
production of antibody	1.03E-09	16
quantity of immunoglobulin	4.11E-09	15
quantity of IgG	6.50E-09	13
cell death of T lymphocytes	9.67E-09	15
differentiation of T lymphocytes	4.36E-08	15
function of T lymphocytes	7.55E-08	13
Rheumatic Disease	4.56E-07	25
expansion of T lymphocytes	5.32E-07	9
proliferation of B lymphocytes	8.67E-07	12
quantity of helper T lymphocytes	9.26E-07	10
immune response of T lymphocytes	1.03E-06	8
quantity of IgG1	3.30E-06	8
rheumatoid arthritis	5.88E-06	18
quantity of IgG2a	6.22E-06	7
differentiation of naive T lymphocytes	1.95E-05	5
proliferation of helper T lymphocytes	7.75E-05	5
differentiation of helper T lymphocytes	1.45E-04	7

c

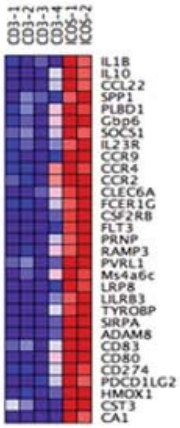

Supplementary Figure 5

Microarray analysis of genes upregulated in CD4$^+$ T cells by costimulation with ICOS.

a, Multiplot of genes upregulated in CD4$^+$ T cells after restimulation with anti-CD3 and anti-ICOS (duplicates) compared to anti-CD3 alone (quadruplicates) as described in **Fig. 4a**. 210 (red) genes upregulated and 9 (blue) genes downregulated after co-ligation of CD3 and ICOS (cut-off 1.5 fold and $P < 0.01$). **b**, Functional analysis performed by Ingenuity pathway analysis (IPA) of 210 genes upregulated by ICOS co-stimulation in **a**. Functional annotations that are related to T-cell activation, differentiation, antibody production and antibody-mediated autoimmune disease with *P* values and numbers of genes are listed. **c**, Heatmap analysis displays 31 genes upregulated in ICOS-activated CD4$^+$ T cells that correlate with systemic autoimmune syndrome revealed by IPA in **b** ($P = 2.65 \times 10^{-11}$).

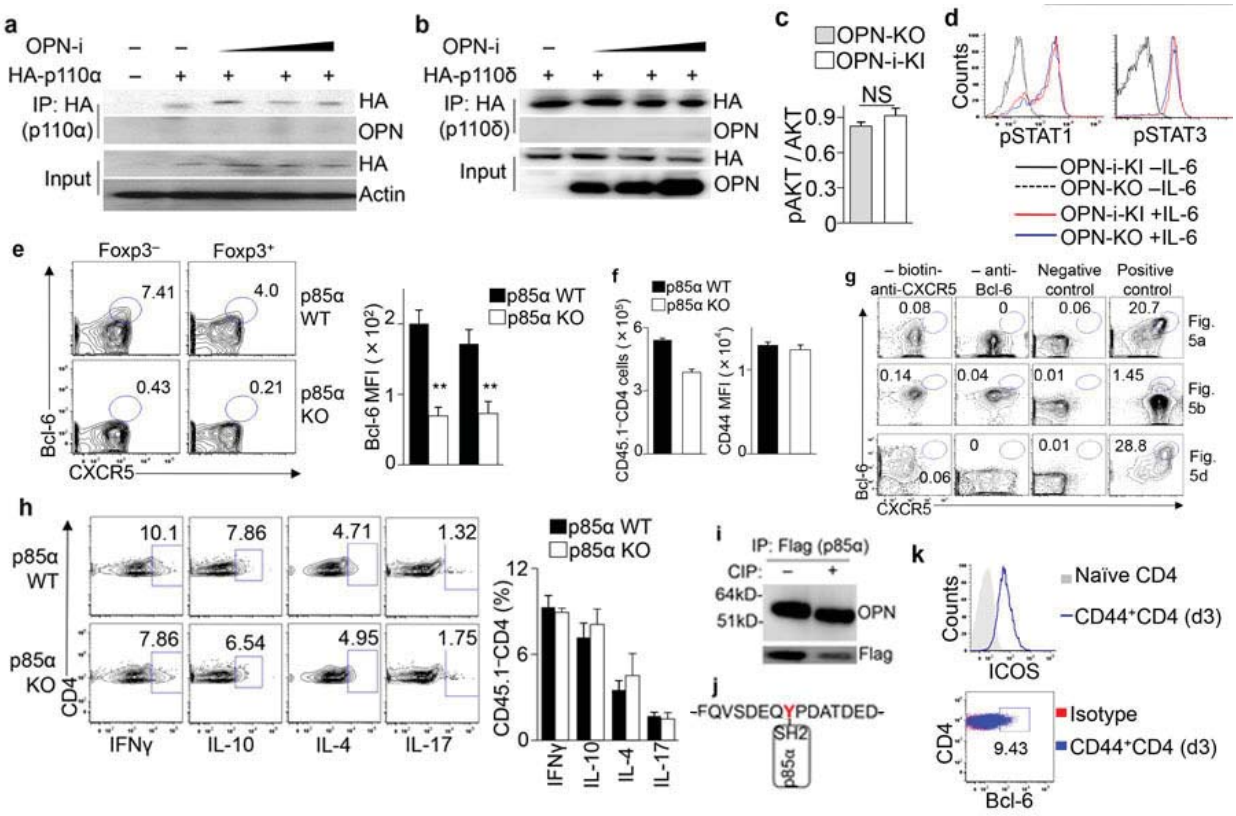

Supplementary Figure 6

OPN-i does not interact with p110, and p85α deficiency does not impair other helper T cell differentiation *in vivo*.

Immunoassay of lysates of 293T cells transfected with plasmids expressing HA-p110α (**a**) or HA-p110δ (**b**) and increasing concentrations of OPN-i, assessed by immunoprecipitation with anti-HA and immunoblot analysis with the indicated Abs. **c**, Purified $CD44^+CD4^+$ T cells from OPN-i-KI or OPN-KO mice 3 d after immunization with KLH and CFA were treated as in **Fig. 4a**. Quantification of ratios of phospho-Akt (pAkt) to total Akt by ELISA from cells after 30 min of crosslinking. **d**, Flow cytometry of splenocytes of OT-II OPN-i-KI or OT-II OPN-KO mice 3 d post-immunization with NP_{13}-OVA in CFA, stimulated with (+) or without (–) IL-6 (20 ng/ml) for 15 min. Overlay of histograms of intracellular phospho-STAT1 and phospho-STAT3 among $CD4^+CD44^+$ T cells. **e**, Flow cytometry of splenocytes from p85α wild-type and p85α KO mice 3 d after injection with KLH and CFA. Numbers indicate percent $Foxp3^-Bcl\text{-}6^+CXCR5^+$ T_{FH} cells and $Foxp3^+Bcl\text{-}6^+CXCR5^+$ T_{FR} cells. Right, Bcl-6 MFI (n = 4 mice per group). $^{**}P < 0.01$ (unpaired two-tailed Student's t-test; error bars, mean ± s.e.m). Data represent two independent experiments. **f**, Quantification of numbers and surface CD44 expression of $CD45.1^-$ $CD4^+$ donor cells from **Fig. 5a**. **g**, Gating controls for defining $Bcl\text{-}6^+CXCR5^+$ $CD4^+$ T_{FH} or T_{FR} cells in **Fig. 5a,b,d**. CXCR5 control: all antibodies except (–) biotin-anti-CXCR5 (streptavidin-APC alone); Bcl-6 control: all antibodies except anti-Bcl-6; in this case, an IgG isotype-matched control for anti-Bcl-6 was used; Negative control: splenic $CD44^{lo}CD4^+$ T cells from B6 mice at day 8 post-injection with KLH in CFA; Positive control: splenic $CD44^{hi}CD25^{med}CD4^+$ T cells from B6 mice at d8 post-immunization with KLH in CFA; or $Bcl\text{-}6^+CXCR5^+$ cells in $CD19^+$ B cells from $Tcr\alpha^{-/-}$ recipients of p85α KO T_{reg} in **Fig. 5b**. **h**, Flow cytometry of donor $CD45.1^-$ $CD4^+$ T cells from **Fig. 5a**, stimulated with PMA and Ionomycin for 5 h. Numbers indicate percent $CD4^+$ T cells expressing intracellular cytokines. Right, frequency of cytokine-producing $CD4^+$ T cells. Data represent two independent experiments with 3-4 mice per group (error bars, mean ± s.e.m). **i**, Immunoassay of lysates of 293T cells transfected with vectors expressing Flag-p85α and OPN-i, treated with calf intestinal phosphatase

(CIP), and assessed by immunoprecipitation with anti-Flag followed by immunoblot analysis. **j**, Diagram of a short sequence motif of OPN with a tyrosine at position 166 that may interact with the p85α SH2 domain. **k**, Expression of surface ICOS receptor and intracellular Bcl-6 in $CD44^{+}CD4^{+}$ T cells from OPN-i-KI mice 3 d after immunization with KLH in CFA.

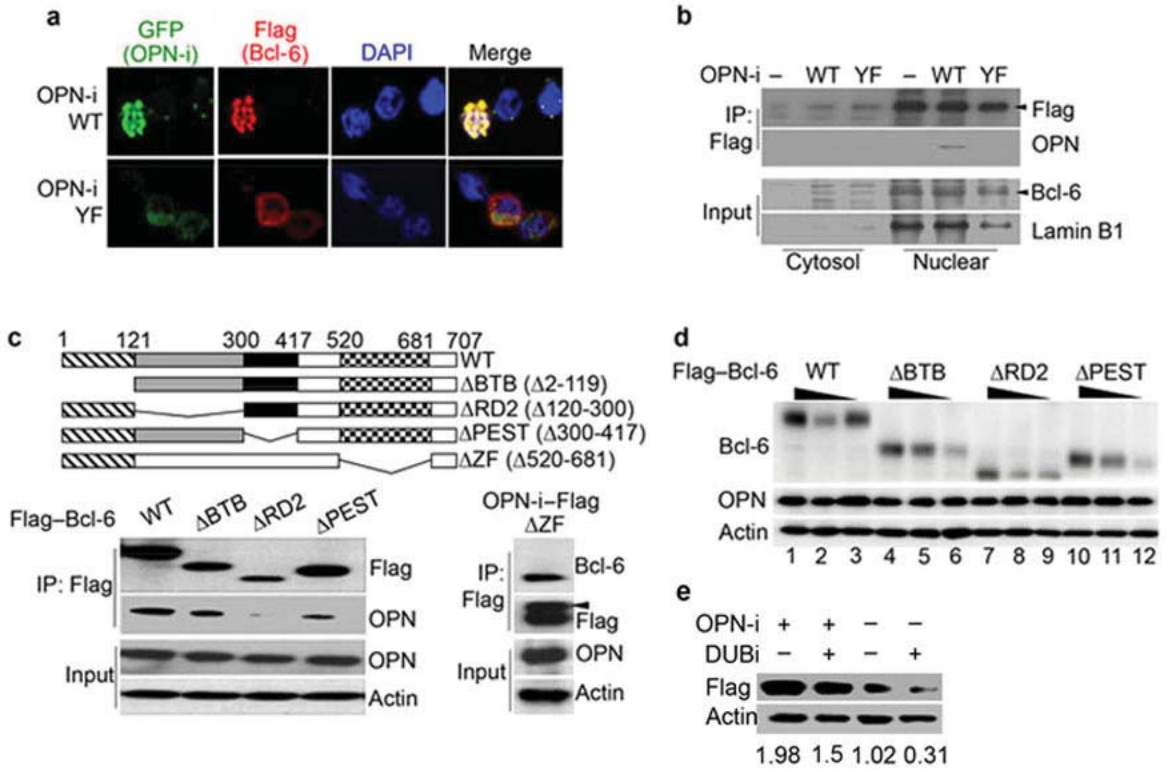

Supplementary Figure 7

Wild-type OPN-i interacts with and stabilizes Bcl-6, but the Y166F OPN-i mutant does not.

a, Confocal microscopy of 293T cells transfected with plasmids encoding p85α, Flag–Bcl-6 and OPN-i–GFP wild-type or OPN-i–GFP Y166F mutant, assessed by pre-extraction of soluble nuclear proteins with 0.5% Triton X-100 after 24 h of transfection followed by immunostaining as indicated. Yellow in the merged image shows colocalization of Bcl-6 and OPN-i wild-type. **b**, Immunoassay of nuclear and cytosolic fractions of 293T cells transfected with plasmids encoding Flag–Bcl-6, OPN-i wild-type or OPN-i Y166F mutant, assessed by immunoprecipitation (IP) with anti-Flag and then immunoblot analysis. **c**, Top, Illustration of Bcl-6 protein deletion mutants. Immunoassay of lysates of 293T cells transfected with plasmids encoding OPN-i and Flag–Bcl-6 wild-type or deletion mutants, assessed by IP and immunoblot analysis as in **b**. Right, immunoassay of lysates of 293T cells transfected with plasmids encoding OPN-i–Flag and Bcl-6 ZF deletion mutant (no Flag tag) followed by IP with anti-Flag and immunoblot with anti-Bcl-6 and anti-Flag. Arrowhead: IgG heavy chain. **d**, Immunoblot analysis of lysates of 293T cells transfected with plasmids encoding OPN-i (100 ng) and graded concentrations of Flag–Bcl-6 wild-type or deletion mutants (lane 1,4,7,10: 450 ng; 2,5,8,11: 300 ng; 3,6,9,12: 150 ng). Cell lysates from lanes 1,4,7,10 were used for immunoassay in **Fig. 7b**. **e**, Immunoblot analysis of lysates of 293T cells transfected with plasmids encoding Flag–Bcl-6 and/or OPN-i, treated with (+) or without (–) DUBi for 8 h, probed with anti-Flag and anti-actin. Below lanes, ratio of Flag (Bcl-6) to actin.

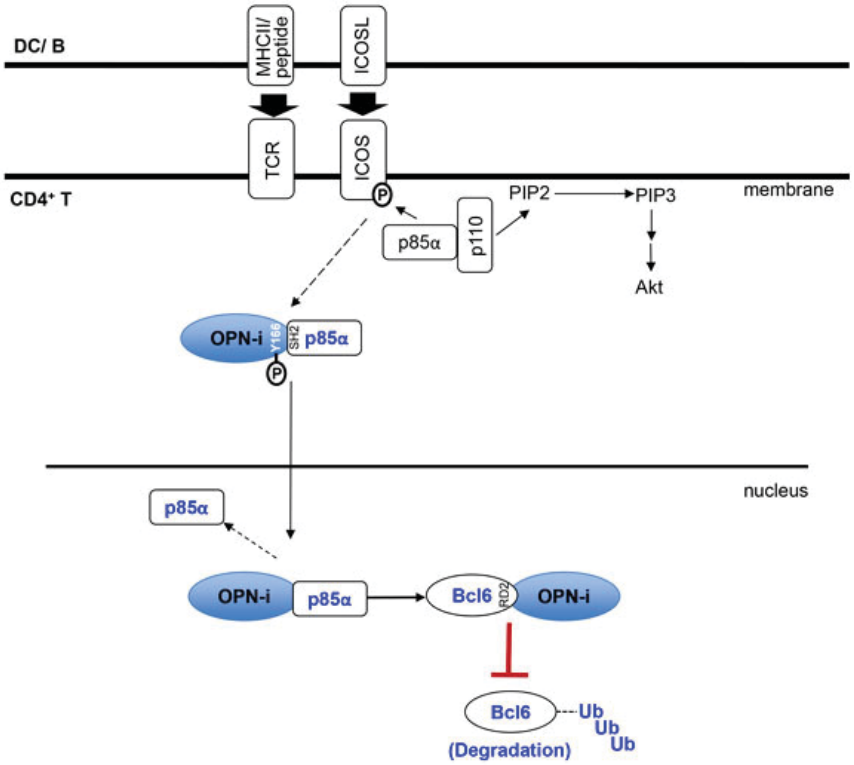

Supplementary Figure 8

Schematic of sustenance of Bcl-6-dependent follicular T cell differentiation mediated by the p85α–OPN-i axis.

Engagement of ICOS and TCR on $CD4^+$ T cells by APC (e.g., DC) promotes p85α–OPN-i complex formation that requires the tyrosine site 166 of OPN-i. p85α chaperones OPN-i entry into the nucleus, where intranuclear OPN-i interacts with Bcl-6 via the sequences within the RD2 and protects Bcl-6 from ubiquitination-mediated degradation. This p85α–OPN-i axis connects ICOS signals to stable Bcl-6 expression (highlighted in blue) and ensures functional follicular T cell differentiation program.